John von Neumann Institute for Computing

Strong Disorder Renormalization Group Calculations of Random Quantum Magnets

Yu-Cheng Lin, Ferenc Iglói, Heiko Rieger

published in

NIC Symposium 2004, Proceedings,
Dietrich Wolf, Gernot Münster, Manfred Kremer (Editors),
John von Neumann Institute for Computing, Jülich,
NIC Series, Vol. **20**, ISBN 3-00-012372-5, pp. 301-310, 2003.

© 2003 by John von Neumann Institute for Computing
Permission to make digital or hard copies of portions of this work for personal or classroom use is granted provided that the copies are not made or distributed for profit or commercial advantage and that copies bear this notice and the full citation on the first page. To copy otherwise requires prior specific permission by the publisher mentioned above.

http://www.fz-juelich.de/nic-series/volume20

Strong Disorder Renormalization Group Calculations of Random Quantum Magnets

Yu-Cheng Lin[1], **Ferenc Iglói**[2,3], **and Heiko Rieger**[4]

[1] Institut für Physik, WA 331, Johannes Gutenberg-Universität
55099 Mainz, Germany
E-mail: lin@uni-mainz.de

[2] Research Institute for Solid State Physics and Optics
1525 Budapest, P.O.Box 49, Hungary
E-mail: igloi@szfki.hu

[3] Institute of Theoretical Physics, Szeged University
6720 Szeged, Hungary

[4] Theoretische Physik, Universität des Saarlandes
66041 Saarbrücken, Germany
E-mail: h.rieger@mx.uni-saarland.de

The strong disorder renormalization group (SDRG), which is devised to study models of strongly disordered quantum magnets at zero and low temperatures, is numerically implemented. Due to the enormous number ($\sim 10^4 - 10^5$) of disorder realization that have to be calculated in order to obtain an acceptable statistics, a parallel computer with trivial farming is optimally suited to perform the calculations. The numerical SDRG is used (A) to study the two-dimensional random Ising ferromagnet in a transverse field close to the quantum critical point at zero temperature, and (B) to study randomly frustrated Heisenberg quantum magnets, also called Heisenberg quantum spin glasses, at zero temperature in 2 and 3 space dimensions. The universal properties found in case (A) are compared with quantum Monte-Carlo simulations, where good agreement is found. Case (B) is mainly *terra incognita* (due to the sign problem occurring in higher dimensional frustrated Heisenberg systems) and can only be compared with small scale exact diagonalization techniques.

1 Introduction

The effect of quenched randomness on disordered quantum magnets close to a quantum phase transition is much stronger than that for classical systems at temperature driven phase transitions. As first observed by McCoy[1] in a somewhat disguised version of a random transverse Ising chain, non-conventional scaling and off-critical singularities that lead to divergent susceptibilities even away from the critical point now appear to be a generic scenario in any dimensions at least in disordered quantum magnets with an Ising symmetry. The reason for this, as pointed out by Fisher only recently, is the behavior governed by a novel fixed point of these systems under renormalization, namely the so-called *infinite randomness fixed point*[2], which is totally determined by the randomness and its geometric properties.

Within this scenario the quantum critical behavior of disordered transverse Ising models is essentially determined by strongly coupled clusters and their geometric properties[2]. Let L be the linear cluster size then it contributes to the low energy spectrum with an exponentially small excitation gap of size $\ln \Delta E \sim L^{-\psi}$, defining the exponent ψ. Moreover,

at the critical point, it will contribute with a magnetic moment of $\mu \sim L^{\Phi\psi}$, defining the exponent Φ. Finally the linear length scale of strongly coupled clusters occurring a distance δ away from the critical point is $\xi \sim |\delta|^{-\nu}$ giving rise to a third scaling exponent ν. All bulk exponents can now be expressed via ψ, ϕ and ν, c.f. $\beta_b/\nu = x_b = d - \phi\psi$, $\nu_{\rm typ} = \nu(1-\psi)$ and in the Griffiths phase $z' \propto \delta^{-\nu\psi}$. For the 1d case, as treated above, it is $\psi = 1/2$, $\phi = (\sqrt{5}+1)/2$ and $\nu = 2$ for uncorrelated disorder.

The basic geometric objects, the strongly coupled clusters, have still to be defined and this will be done within a renormalization group scheme. However, for site or bond *dilution* it is immediately obvious what these clusters are: simply the connected clusters. Hence the critical exponents defined above are directly related to the classical percolation exponents: Let $\delta = p - p_c$ be the distance from the percolation threshold, $\nu_{\rm perc}$ the exponent for the typical cluster size, $D_{\rm perc}$ the fractal dimension of the percolating cluster, $\beta_{\rm perc}$ the exponent for the probability to belong to the percolating cluster. Then one has for the critical exponents defined above

$$\nu = \nu_{\rm perc}\ , \quad \psi = D_{\rm perc}\ , \quad \phi = (d - \beta_{\rm perc}/\nu_{\rm perc})/D_{\rm perc}. \tag{1}$$

Next we consider the question, what happens for generic disorder (i.e. no dilution, but random bonds and/or fields) and we consider the random transverse Ising model (RTIM) defined by the Hamiltonian

$$H = -\sum_{\langle i,j\rangle} J_{ij}\sigma_i^z\sigma_j^z - \sum_i h_i\sigma_i^x. \tag{2}$$

Here the $\{\sigma_i^\alpha\}$ are Pauli spin matrices, and the nearest neighbor interactions J_{ij} and transverse fields h_i are both independent random variables distributed uniformly: $\pi(J_{ij}) = 1$ for $0 < J_{ij} < 1$ and 0 otherwise, $\rho(h_i) = h^{-1}$ for $0 < h_i < h$ and 0 otherwise. In one space dimension this model has been investigated intensively over the recent years, and many analytical as well as numerical tools are on hand to analyze it. Beyond the simple one-dimensional geometry one has to rely on numerical techniques like quantum Monte-Carlo simulations[6,7] or the numerical implementation of the renormalization group scheme, which we outline in the next section.

2 The SDRG Method for Random Transverse Ising Systems

The strategy of the renormalization-group á la Dasgupta and Ma[3] is to decrease the number of degrees of freedom and reduce the energy scale by performing successive decimation transformation in which the largest element of the set of random variables $\{h_{i;}\, J_{ij}\}$ at each energy scale is eliminated and weaker effective couplings are generated by perturbation theory.

The renormalization-group procedure is as follows: find the strongest coupling

$$\Omega \equiv \max\{J_{ij},\, h_i\}.$$

If $\Omega = J_{ij}$, then the neighboring transverse fields $h_{i,\,j}$ can be treated as a perturbation to the term $-J_{ij}\sigma_i^z\sigma_j^z$ in the Hamiltonian (2); The two spins involved are joined together into a spin cluster with an effective transverse field

$$\widetilde{h}_{(ij)} \approx \frac{h_i h_j}{J_{ij}}$$

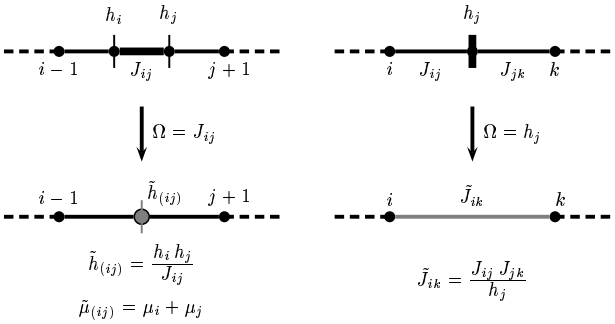

Figure 1. Schematic of renormalization-group decimation for spin chains.

and an effective magnetic moment

$$\widetilde{\mu}_{(ij)} = \mu_i + \mu_j.$$

The bonds of the new cluster $\widetilde{\sigma}_{(ij)}$ with other clusters σ_k are

$$\widetilde{J}_{(ij)k} \approx \max(J_{ik},\, J_{jk}).$$

If instead $\Omega = h_j$, then the associated spin σ_j is eliminated and effective bonds between each pair of its neighboring spins are generated by second-order perturbation theory. The strength of the effective bonds for each pair $(i,\, k)$ is

$$\widetilde{J}_{ik} \approx \max(J_{ik}\,,\, \frac{J_{ij}J_{jk}}{h_j}),$$

where the J_{ik} are the bonds that may have already been present. This procedure is sketched for the $1d$ case in fig. 1.

At each stage of the RG, an effective field (bond) is a ratio of a product of some number f of original fields (bonds)to a product of original $f-1$ bonds (fields). The f grows under renormalization at criticality. As a result, the log-field and log-bond distributions $R_\Omega(\ln \widetilde{h})$ and $P_\Omega(\ln \widetilde{J})$ become broader and broader under renormalization if the critical point is approached. This increasing width of the field and bond distributions reduces the errors made by the second-order perturbation approximation. The RG becomes thereby asymptotically exact.

The RG can be carried out analytically in one space dimension[4,5], therefore we can use the $1d$ case as a simple check for our numerical implementation. In Fig. 2 we show the probability distribution of the logarithm of the last remaining cluster field at the critical point $h_0 = 1$, which scales, according to Fig. 2 like $\ln \Omega L^{-1/2}$, where L is the system size. From this one concludes that the exponent ψ defined in the introduction, is given by $\psi = 1/2$. Inspecting the number of active spins in the last remaining cluster at the critical point we the size dependence $\mu \sim L^{0.81}$ from Fig. 3, and thus $\phi \approx 1.62$, which agrees well with the analytical predictions[4,5].

Next we present our results for the two-dimensional case, where we kept *all* bonds generated during renormalization. The RG scheme for the two-dimensional case is depicted in Fig. 4.

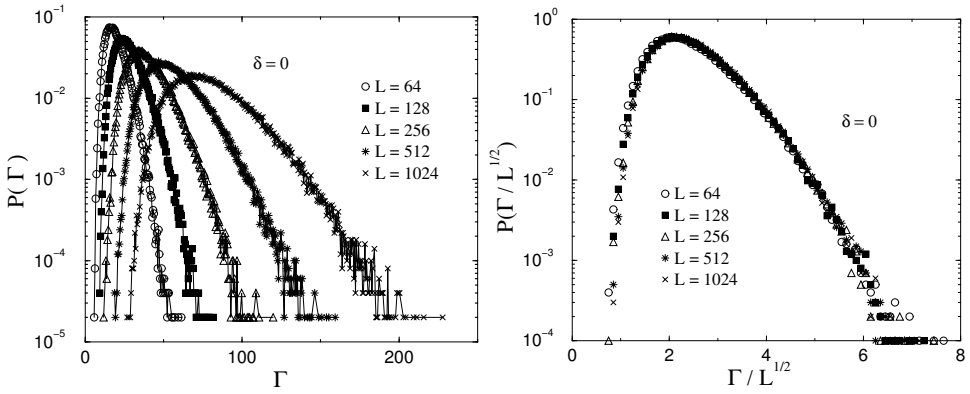

Figure 2. **Left:** Distribution of the logarithmic strength of the last remaining cluster fields, $\Gamma \equiv \ln(\frac{\Omega_0}{\Omega_{\tilde{h}}})$, for the one-dimensional ($d = 1$) RTIM. The distribution gets broader on a logarithmic scale with increasing system size, indicating a infinite dynamical exponent z. The data are obtained from 100 000 samples for each system size. **Right:** Scaling of the data in the left figure, assuming the exponential scaling form obtained from the analytical work.[5,4]

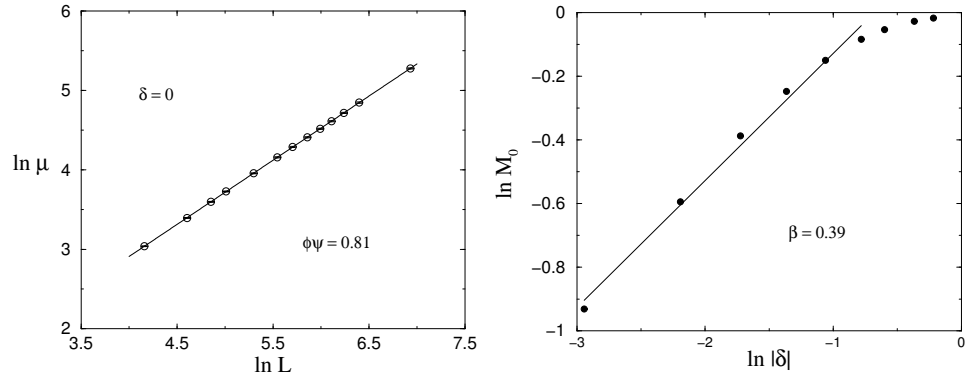

Figure 3. **Left:** Scaling of the number of active spins (proportional to average magnetic moment per spin, μ) in the last remaining spin cluster at the critical point for the one-dimensional ($d = 1$) RTIM. We find $\mu \sim L^{0.81}$ implying $\phi \approx 1.62$. **Right:** In the ordered phase ($\delta < 0$), the spontaneous magnetization scales as $M_0 = |\delta|^\beta$ with $\beta \approx 0.39$. This numerical estimate of β is in agreement with the analytical prediction: $\beta = \frac{3-\sqrt{5}}{2}$. Our data are obtained by averaging over 100 000 samples of size $L = 1024$.

We obtain a critical field approximately at $h_0 = 5.3$ by applying the criterion that field and bond distribution should behave similar (as for the 1d case and the double chain[8]). The scaling of the last log-field distribution yields $\psi \approx 0.5$ and the scaling plot of the number of the active spins in the last remaining cluster yields $\phi \approx 2.0$ and $\mu \sim L^{1.06}$, which agrees well with the estimates from quantum Monte Carlo simulations[6,7].

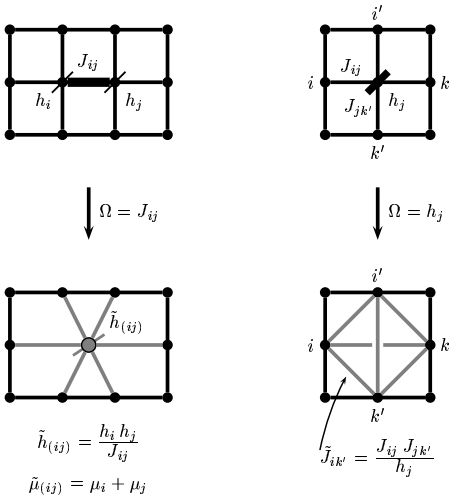

Figure 4. Schematic of renormalization-group decimation for the two-dimensional (square) lattice used in the numerical calculations.

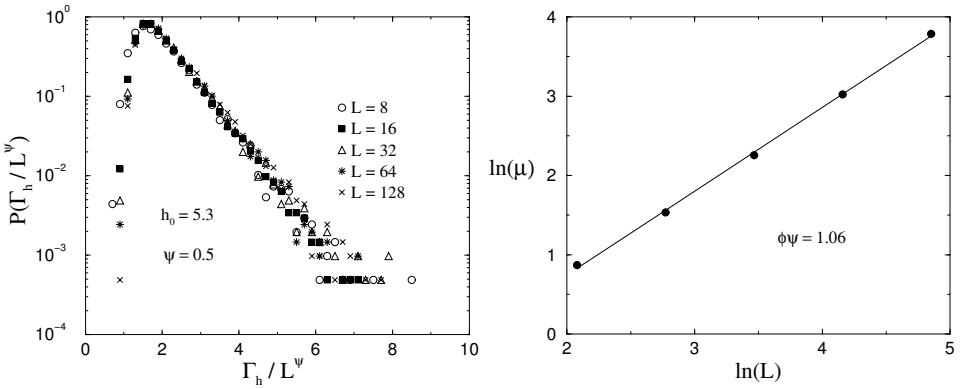

Figure 5. **Left:** Scaling of the log-fields at the last stage of the RG at the estimated to critical point $h_0 = 5.3$ for RTIM on the square lattice ($d = 2$). **Right:** A scaling plot of the number of the active spins in the last remaining cluster at the estimated critical point of the RTIM square lattice.

3 Random Bond Heisenberg Systems

The Hamiltonian describing a spin-1/2 Heisenberg system is given by

$$H = \sum_{\langle ij \rangle} J_{ij} \mathbf{S}_i \mathbf{S}_j \ , \tag{3}$$

where the sum is over all nearest neighbor pairs $\langle ij \rangle$ on a regular lattice and the exchange couplings J_{ij} are random variables indicating either a ferromagnetic (F), $J_{ij} < 0$, or anti-ferromagnetic (AF) interaction, $J_{ij} > 0$. In all interesting cases a mixture of ferromag-

netic and anti-ferromagnetic interactions (on some lattices even the presence of only anti-ferromagnetic couplings) produces frustration which renders an efficient quantum Monte-Carlo investigation of such a system impossible. An alternative tool for investigation in case of strongly disordered systems is the SDRG.

The basic ingredient of the SDRG method in Heisenberg models is a successive decrease of the energy scale of excitations via a successive decimation of couplings. We start with a $S = 1/2$ HAF model in which the the strongest coupling is, say J_{23}, the one between lattice sites 2 and 3 (c.f. Fig. 6). If J_{23} is much larger than its neighboring couplings J_{12}, J_{13}, J_{24} and J_{34}, the spins at 2 and 3 form an effective singlet and are decimated. The effective coupling between the remaining sites, 1 and 4 in second order perturbation theory is given by:

$$\tilde{J}_{14}^{\rm eff} = \lambda \frac{(J_{12} - J_{13})(J_{34} - J_{24})}{J_{23}}, \quad \lambda(S = 1/2) = 1/2 \; . \tag{4}$$

In a chain geometry the couplings J_{13} and J_{24} would not be present and the resulting RG flow always generates AF couplings. However, for extended, not strictly $1d$ objects, some of the generated new couplings can be ferromagnetic (e.g. if $J_{12} < J_{13}$ and $J_{34} > J_{24}$ or vice versa) and therefore the decimation rules have to be extended. If at one RG step an F bond turns out to be the strongest one, its decimation will lead to an effective spin $\tilde{S} = 1$. In the following steps, the system will renormalize to a set of effective spins of different magnitude interacting via F *and/or* AF couplings.

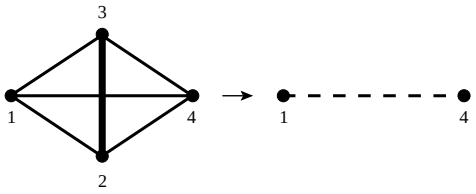

Figure 6. Singlet formation and decimation for a spin configuration that does not have a chain topology and typically occurs in higher dimensional systems.

For higher dimensional systems, the basic decimation processes are the singlet formation in Eq.(4) and the effective spin (cluster) formation. To specify the latter, let us consider three spins S_1, S_2 and S_3 with interactions fulfilling $|J_{23}| \gg |J_{12}|, |J_{13}|$. In the action of the RG, the two original spins S_2 and S_3 form a new effective spin of magnitude $\tilde{S} = |S_2 \pm S_3|$ representing the total spin of the ground state in the two-spin Hamiltonian $H_{23} = J_{23}\mathbf{S}_2\mathbf{S}_2$, where the positive (negative) sign refers to an F (AF) coupling. The corresponding energy gap, Δ, between the ground state and the first excited state in the Hamiltonian H_{23} is given by $\Delta = |J_{23}|(S_2 + S_3)$ and $\Delta = J_{23}(|S_2 - S_3| + 1)$, for an F and AF coupling, respectively. If $J_{23} > 0$ (AF) and $S_2 = S_3$, it follows an effective singlet formation as described above. If $\tilde{S} \neq 0$, within first order perturbation theory the new coupling between S_1 and $\tilde{S}_{23}$ is given by

$$\tilde{J}^{\rm eff} = c_{12}J_{12} + c_{13}J_{13} \; , \tag{5}$$

with

$$c_{12} = \frac{\tilde{S}(\tilde{S}+1) + S_2(S_2+1) - S_3(S_3+1)}{2\tilde{S}(\tilde{S}+1)}$$

and

$$c_{13} = \frac{\tilde{S}(\tilde{S}+1) + S_3(S_3+1) - S_2(S_2+1)}{2\tilde{S}(\tilde{S}+1)}.$$

At each RG step, we find the pair of the spins with the largest energy gap Δ that sets the energy scale, Ω, and decimate them according to renormalization rules described in (4) or (5).

The fixed point of the RG transformation for lattices that do *not* have a chain geometry may depend on their topology, the original distribution of bonds, the strength of the disorder, etc. Here we briefly summarize the results for Heisenberg quantum spin glasses, results for other quantum Heisenberg models, like ladders and two-dimensional models on various lattices are reported by us in Ref. 9, 10.

3.1 Scaling Laws

In the case of the random AF chain (which does neither have F bonds nor frustration), the RG procedure described above runs into an infinite randomness fixed point (IRFP) corresponding to a random singlet phase. In this phase the renormalized clusters are singlets, thus the total magnetic moment is zero, and the energy and length scales are related via $-\ln\Omega \sim L^{1/2}$, which means that the dynamical exponent is formally infinite.

A dimerized $S = 1/2$ chain with random AF even ($J_{\rm e}$) and odd ($J_{\rm o}$) couplings shows dimer order and the low-energy behavior is controlled by a *random dimer fixed point* at which the dynamical exponent, z, is finite and a continuously varying function of the strength of the dimerization measured by $\delta_{\rm dim} = [\ln J_{\rm e}]_{\rm av} - [\ln J_{\rm o}]_{\rm av}$. This random dimer phase is a Griffiths phase. At this Griffiths fixed point (GFP), the distribution of gaps of finite chains of length L obeys

$$P_L(\Delta) = L^z \tilde{P}(L^z\Delta) \sim L^{z(1+\omega)}\Delta^{\omega}\ , \tag{6}$$

which is characterized by the gap exponent, ω. As a consequence of Eq.(6), which holds in any dimension, several dynamical quantities at a GFP are singular and the characteristic exponents can all expressed via ω. For example the susceptibility χ, the specific heat C_v (at a small temperatures T), and the magnetization m (in a small field h), behave as: $\chi(T) \sim T^{-\omega}$, $C_v(T) \sim T^{\omega+1}$, and $m(h) \sim h^{\omega+1}$. In the Griffiths phase there is a simple relation between the dynamical exponent, z, and the gap exponent, ω, which can be obtained by the following phenomenological consideration: If the Griffiths singularities are due to rare events (produced by the couplings) that give rise to *localized* low-energy excitations, the gap distribution should be proportional to the volume, $P_L(\Delta) \sim L^d$. From Eq.(6) then follows $z = d/(1+\omega)$, which is consistent with the exact result in the random dimer phase. However, if the low-energy excitations are *extended* this relation might not hold, as we will see for randomly frustrated Heisenberg models in $3d$.

In a spin chain with mixed F and AF couplings[10], large effective spins, $S_{\rm eff}$, are formed at the fixed point of the transformation. The size of of these spin clusters scales with the

fraction of surviving sites during decimation, $1/N$, as:

$$S_{\rm eff} \sim N^{\zeta} \ . \tag{7}$$

The following random walk argument gives $\zeta = 1/2$. The total moment of a typical cluster of size N can be expressed as $S_{\rm eff} = |\sum_{1=1}^{N} \pm S_i|$, where neighboring spins with F (AF) couplings enter the sum with the same (different) sign. If the position of the F and AF bonds are uncorrelated and if their distribution is symmetrical, one has $S_{\rm eff} \propto N^{1/2}$, i.e. Eq.(7) with $\zeta = 1/2$.

A non-trivial relation constitutes the connection between the energy scale Ω and the size of the effective spin:

$$S_{\rm eff} \sim \Omega^{-\kappa} \ . \tag{8}$$

Comparing Eq.(7) with Eq.(8), the relation between the length scale $L \sim N^{1/d}$ ($d = 1$) and the energy scale is: $\Omega \sim L^{-z}$, $z = \frac{d\zeta}{\kappa} = \frac{1}{2\kappa}$, where z is the dynamical exponent. The distribution of low-energy gaps, $P_L(\Delta)$, has the same power-law form as in Eq.(6). Therefore from the scaling behavior of $P_L(\Delta)$ the gap exponent, ω, and the dynamical exponent, z, can be obtained. Due to the large moment formation the singularities of the dynamical quantities are different from those in the random dimer phase. In d-dimensions one obtains[10]:

$$\chi(T) \sim T^{-1},\ C_v(T) \sim T^{2\zeta(\omega+1)} |\ln T|,\ m(h) \sim h^{\frac{\zeta(1+\omega)}{1+\zeta(1+\omega)}} \ , \tag{9}$$

thus the singularities involve both exponents ζ and ω.

3.2 2d

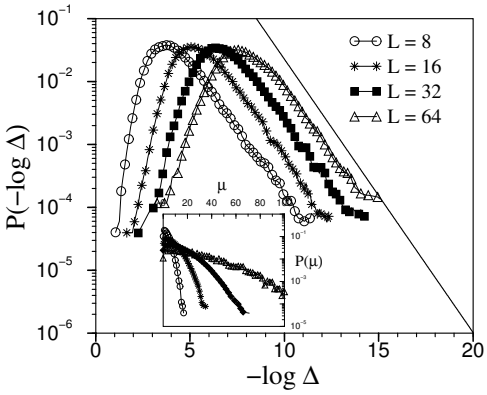

Figure 7. Probability distribution of the energy gap on the square lattice with mixed F and AF bonds following a Gaussian distribution with $\sigma = 1$. (The slope of the straight line is -1). Inset: Distribution of the spin moments.

Here we discuss briefly the Heisenberg model on the square lattice with a random mixture of F and AF couplings. This is a model for a quantum spin glass and we denote the corresponding fixed point as spin glass fixed point (SGFP), although we do not explicitely

check for the existence of proper spin glass order in the ground state (for instance via the calculation of the Edwards-Anderson spin glass order parameter[11]). First we report the results for a Gaussian distribution of the couplings (J_{ij}) with mean zero and variance 1. For this case the distributions of the gaps and of the effective spin moments are shown in Fig. 7.

The gap-distributions for different finite sizes have a very similar structure: they are merely shifted to each other by a constant proportional to $\ln L$. The slope of the low-energy tail is well described by $P(\Delta) \sim \Delta^{\omega}$ with $\omega = 0$. On the other hand, the distribution of the effective spin moments in the inset to Fig. 7 shows a tendency to broaden with increasing system size and its average value has a linear L dependence, $[\mu_L]_{\rm av} \approx .42L$. Therefore the moment exponent ζ in $[\mu_L]_{\rm av} \propto L^{\zeta}$. is $\zeta = 1/2$. Similarly the dynamical exponent is given by $z = 2$.

We have repeated the above analysis using a symmetric rectangular both for the $S = 1/2$ and the $S = 1$ models and we obtained the same critical exponents as in the Gaussian case. Thus we can conclude that the low-energy behavior in randomly frustrated $2d$ models is controlled by the same SGFP, independent of the type of randomness and spin value.

3.3 3d

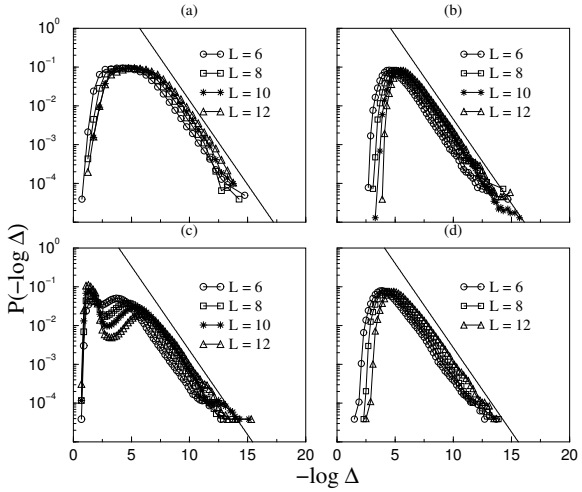

Figure 8. Probability distribution of the energy gap on the cubic lattice with mixed F and AF bonds. (a) Gaussian distribution, $\sigma = 1$; (b) symmetric rectangular distribution: $P_r(J) = \Theta(1/2 + J)\Theta(1/2 - J)$; (c) asymmetric rectangular distribution: $P_r(J) = \Theta(J - r + 1/2)\Theta(r + 1/2 - J)$ with $r = 0.25$; (d) $S = 1$ symmetric rectangular distribution. The low-energy tails of the gap distributions for all cases, indicated by straight lines, have a slope -1, corresponding to $\omega = 0$.

For the calculations in $3d$ that we present now we considered only systems of linear size $L = 6, 8, 10$ and 12, in some cases we went up to $L = 16$. Larger system sizes were computationally not feasible. The typical number of realizations were several ten-thousand

for each point. Due to the smaller system sizes the finite-size effects in $3d$ are stronger than in $2d$. These finite size effects turned out to be too strong in the random HAF on the cubic lattice for a safe estimate for the gap exponent. We can, however, conclude that there is no large spin formation and the low-energy behavior is controlled by a conventional GFP.

We have studied models with mixed F and AF couplings for different form of initial randomness (Gaussian, symmetric and asymmetric rectangular) and for comparison calculations on the $S = 1$ model are also performed. The calculated distributions of the gaps are presented in Fig. 8.

As seen in Fig. 8 the slopes of the low-energy tail of the gap-distributions are approximately constant, and for our finite systems they are consistent with a vanishing gap exponent: $\omega \approx 0$ in $d = 3$. During renormalization, as in $2d$, there is a large spin formation and the corresponding moment exponent is $\zeta = 0.55$, for symmetric distributions (Gaussian and rectangular) and $\zeta = 0.58$ for the asymmetric rectangular distribution. Thus ζ appears to be close to $1/2$ in both cases. We have also studied the scaling behavior of the reduced gap distribution, $\tilde{P}(L^z\Delta) = L^{-z}P_L(\Delta)$. and obtain $z \approx 3/2$ independently of the disorder distribution. The scaling curves seem to tend to a finite limiting value at $\Delta = 0$, implying a gap exponent $\omega \approx 0$. We can thus conclude that — within the range of validity of the SDRG method — the relation $z = d/(1 + \omega)$, valid for RTIMs and non-frustrated Heisenberg models, is not valid for frustrated 3d Heisenberg models.

Acknowledgments

The computations were performed with a grant of computer time provided by the NIC at the Research Centre Jülich. This work has been supported by a German-Hungarian exchange program (DAAD-MÖB).

References

1. B. M. McCoy, Phys. Rev. Lett. **23**, 383 (1969).
2. D. S. Fisher, Physica A **263**, 222 (1999).
3. C. Dasgupta and S. K. Ma, Phys. Rev. B **22**, 1305 (1980).
4. D. S. Fisher, Phys. Rev. Lett. **69**, 534 (1992); Phys. Rev. B **51**, 6411 (1995).
5. F. Iglói and H. Rieger, Phys. Rev. B **57**, 11404 (1998).
6. C. Pich, A. P. Young, H. Rieger, and N. Kawashima, Phys. Rev. Lett. **81**, 5916 (1998).
7. H. Rieger and N. Kawashima, Europ. Phys. J. B **9**, 233 (1999).
8. Y.-C. Lin, N. Kawashima, F. Iglói, and H. Rieger, Prog. Theor. Phys. Suppl. **138**, 479 (2000).
9. R. Mélin, Y.-C. Lin, P. Lajkó, H. Rieger, and F. Iglói, Phys. Rev. B **65**, 104415 (2002).
10. Y.-C. Lin, R. Mélin, H. Rieger and F. Iglói, Phys. Rev. B **68**, 024424 (2003).
11. For a review see e.g.: H. Rieger and A. P. Young, *Quantum Spin Glasses*, Lecture Notes in Physics **492**, in "Complex Behaviour of Glassy Systems", p. 254, ed. J.M. Rubi and C. Perez-Vicente (Springer Verlag, Berlin-Heidelberg-New York, 1997).